

## Filtering Noncorrelated Noise in Impedance Cardiography

Allan Kardec Barros, Makoto Yoshizawa, and Yoshifumi Yasuda

**Abstract**—Impedance cardiography (ICG) may be altered by noises as respiration and movement artifacts, mainly during exercise. In this work, a scaled Fourier linear combiner (SFLC) event-related to the R-R interval of ECG is proposed. It estimates the deterministic component of the impedance cardiographic signal and removes the noises uncorrelated to this interval. The impedance cardiographic signal is modeled as Fourier series with the coefficients estimated by the least mean square (LMS) algorithm. Simulations have been carried out to evaluate the filter performance for different noise conditions. Moreover, the method capability to remove uncorrelated noises was also examined in physiological data obtained in rest and exercise, by synchronizing respiration and pedaling with a metronome. Analyzing the ICG power spectrum, it was concluded that the proposed filter could remove the noises that are not synchronized with heart rate.

### I. INTRODUCTION

Assessing the cardiac status using impedance cardiography (ICG) has been the scope of hundreds of works because of its relatively simple, atraumatic, repeatable, cost-effective, and noninvasive procedure on a beat-by-beat basis, since the early works of Patterson *et al.* [10] and Kubicek *et al.* [8], whose method uses the ICG first derivative  $dZ/dt$  to calculate the stroke volume and cardiac output. However, the respiratory components and movement artifacts cause changes in the baseline of the signal that may produce measurement errors. First, breath holding was suggested to eliminate the respiratory components [4], [11], but it can alter the stroke volume during measurements. Ensemble averaging was also proposed [9], however, it eliminates the beat-by-beat characteristic of the cardiac output since each recurrence was constructed by averaging five beats.

Recently, filtering techniques were proposed to eliminate the noises caused by respiration. Yamamoto *et al.* [17] suggested a narrow band-pass filter around the cardiogenic frequency, but the filter eliminates the high frequency components of the cardiac signal and has a phase distortion. Eiken and Segerhammer [3] have developed a moving-window technique to identify the breathing artifacts. Raza *et al.* [13] proposed a high-pass third-order Butterworth filter with voluntary cardiorespiratory synchronization (VCRS) using forward and backward filtering to eliminate the phase distortion caused by the infinite impulse response (IIR) filter.

However, there is still the problem of movement artifacts, whose spectra are unknown and may sometimes overlap the signal spectra. One solution to eliminate these movement artifacts is using adaptive filters where, to a certain extent, *a priori* knowledge of the signal statistics is not necessary. Adaptive estimators allow the tracking of the dynamical variations and reduce the noise uncorrelated to the signal. The adaptive filter is based on the adaptive linear combiner [15] (see Fig. 1) with a primary input  $d_k$ , which is the signal to be filtered, and a reference input vector—a vectorial base  $[x_{1,k}, x_{2,k}, \dots, x_{2H,k}]^T$ , producing the output  $y_k$  that estimates the signal of interest  $s_k$ . Laguna *et al.* [6] used a transversal filter with an impulse correlated

Manuscript received January 19, 1994; revised November 21, 1994.

A. K. Barros is with the Department of Knowledge-Based Information Engineering, Toyohashi University of Technology, Toyohashi 441, Japan.

M. Yoshizawa is with the Department of Electrical Engineering, Graduate School of Information Science, Tohoku University, Sendai 980-77, Japan.

Y. Yasuda is with the Research Center of Physical Fitness, Sports and Health, Toyohashi University of Technology, Toyohashi 441, Japan.

IEEE Log Number 9408349.

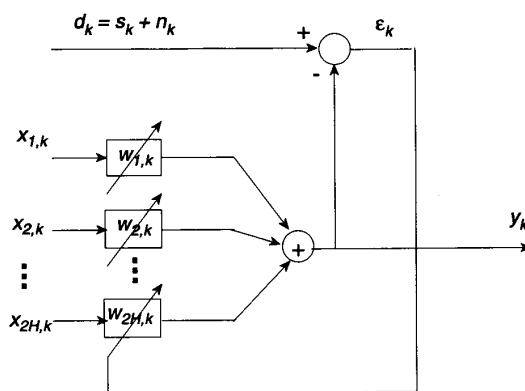


Fig. 1. Block diagram of the adaptive filter.  $s_k$  is the deterministic signal,  $n_k$  is the noise uncorrelated with  $s_k$ .  $[x_{1,k}, x_{2,k}, \dots, x_{2H,k}]^T$  is the reference vector.

to the signal as the reference input; Vaz and Thakor [14] used sine and cosine waves as the reference input in a Fourier linear combiner (FLC) to estimate evoked potentials. It is assumed that the signal is well defined in each recurrence with a constant number of samples. This assumption has a low-pass filtering effect if there are errors in the occurrence time estimation [7].

We propose a scaled Fourier linear combiner (SFLC) to estimate the impedance cardiographic signal with reference inputs related to the R-R intervals of ECG. We use a scaling factor in the reference inputs to have more flexibility than the Fourier linear combiner (FLC) proposed by Vaz and Thakor [14]. Also, we do not assume a constant number of samples in each recurrence because the R-R interval changes during different phases of the respiration cycle [16]. Assuming the interval variation from the  $R$  peak of ECG to the  $dZ/dt$  peak (the maximum value of ICG first derivative within a cardiac cycle) proportional to the R-R interval, the constant number of samples assumption would result in the low-pass filtering effect described by Jané *et al.* [7].

### II. METHODS

#### A. The Adaptive Filter

The adaptive filter at the  $k$ -th iteration has one primary input  $d_k$  composed of the signal of interest  $s_k$  contaminated by a noncorrelated noise  $n_k$  (refer to Fig. 1). Let  $m = 1, 2, \dots, N$  be the beat number index (here, we use the term *beat* to refer to the R-R interval),  $L_m$  be the number of samples at the  $m$ -th beat, and  $l = 1, 2, \dots, L_m$  be the sample index within that beat. Thus, the iteration number  $k$  can be expressed as a function of  $m$  and  $l$  by  $k(m, l) = \sum_{j=1}^{m-1} L_j + l$ . We define the reference signal  $x_{i,k(m,l)}$  as

$$x_{i,k(m,l)} = \begin{cases} \frac{1}{\sqrt{H}} \sin(2\pi \frac{il}{L_m}); & i = 1, 3, 5, \dots, 2H-1 \\ \frac{1}{\sqrt{H}} \cos(2\pi \frac{(i-1)l}{L_m}); & i = 2, 4, 6, \dots, 2H \end{cases} \quad (1)$$

where  $H$  is the number of harmonics required to reconstruct the signal. For simplicity,  $k(m, l)$  will be denoted as  $k$  below. The reference inputs compose a vector  $\mathbf{X}_k = [x_{1,k}, x_{2,k}, \dots, x_{2H,k}]^T$ , and  $\mathbf{W}_k = [w_{1,k}, w_{2,k}, \dots, w_{2H,k}]^T$  is the weight vector. The output

$y_k$  is equal to the inner product of  $\mathbf{X}_k$  and  $\mathbf{W}_k$  as

$$y_k = \mathbf{X}_k^T \mathbf{W}_k = \mathbf{W}_k^T \mathbf{X}_k. \quad (2)$$

Defining the input correlation matrix as  $\mathbf{R} = E[\mathbf{X}_k \mathbf{X}_k^T]$  and the cross-correlation vector  $\mathbf{P} = E[d_k \mathbf{X}_k^T]$ , we have the mean square error (MSE) as (further reference can be found in [6] and [15])

$$\xi = E[(d_k - y_k)^2] = E[d_k^2] - 2\mathbf{P}^T \mathbf{W} + \mathbf{W}^T \mathbf{R} \mathbf{W}. \quad (3)$$

Thus, from (1) we have  $\mathbf{R} = \frac{1}{2H} \mathbf{I}$ .

In a given period  $L_m$ , the signal  $s_k$ , which has a limited bandwidth up to the  $H$ -th harmonic frequency, can be estimated up to this harmonic  $H$  in Fourier series as

$$s_k = \sum_{l=1}^H A_l \cos\left(2\pi \frac{l}{L_m} k\right) + \sum_{l=1}^H B_l \sin\left(2\pi \frac{l}{L_m} k\right) \quad (4)$$

given that  $H < L_m/2 - 1$  [13].

The optimum vector that minimizes the MSE is the Wiener weight vector, given by

$$\mathbf{W}_0 = \mathbf{R}^{-1} \mathbf{P}. \quad (5)$$

When the weight  $\mathbf{W}_k$  converges to the Wiener solution, we have  $y_k = \mathbf{W}_0^T \mathbf{X}_k = s_k$ . We can observe that, in steady-state, the deterministic signal  $s_k$  is well estimated by the SFLC.

The Widrow-Hoff least mean square (LMS) algorithm is given by

$$\mathbf{W}_{k+1} = \mathbf{W}_k - 2\mu(d_k - y_k)\mathbf{X}_k \quad (6)$$

where  $\mu$  is the factor which controls the stability and the rate of convergence. The misadjustment  $\mathbf{M}$  measures how close the LMS algorithm approaches the Wiener solution

$$\mathbf{M} = \frac{E[(s_k - y_k)^2]}{E[n_k^2]}. \quad (7)$$

An approximate misadjustment is given by  $\mathbf{M} = \mu \text{tr}[\mathbf{R}]$  (refer to [15]). Then, for this case,  $\mathbf{M} = \mu$ . From (7) and (3), the MSE in steady-state will be

$$\xi = E[n_k^2](1 + \mathbf{M}) = E[n_k^2](1 + \mu). \quad (8)$$

The convergence of the LMS algorithm depends on the gain constant  $\mu$  satisfying [5]

$$0 < \mu < \frac{1}{3\text{tr}[\mathbf{R}]} = \frac{1}{3} \quad (9)$$

and the time constant for the learning curve with equal eigenvalues [15] is

$$\tau_{\text{mse}} = \frac{2H}{4\mu \text{tr}[\mathbf{R}]} = \frac{H}{2\mu} \quad (10)$$

where  $\tau_{\text{mse}}$  is expressed as a number of iterations of the adaptive process.

From these results, with  $\mathbf{M} = \mu$  and  $\tau_{\text{mse}}$  inversely proportional to  $\mu$ , a trade-off takes place. For a smaller misadjustment, smaller  $\mu$  would be desired, but then  $\tau_{\text{mse}}$  increases. Thus, the choice of  $\mu$  is a compromise between less misadjustment and fast convergence. If the signal under study is stationary,  $\mu$  can be chosen using the method suggested by Bershad [1].

These calculations for MSE are made with the assumption that, after the harmonic  $H$ , the signal power spectrum becomes negligible compared with the spectrum up to the harmonic  $H$  so that (4) holds.

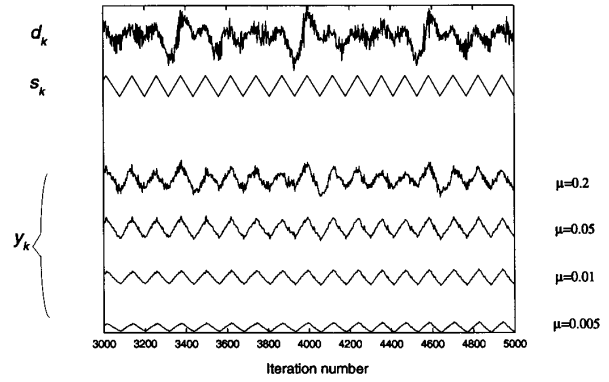


Fig. 2. Simulation using a triangular wave  $s_k$  contaminated by a noise  $n_k$ .  $d_k = s_k + n_k$ . The filter output  $y_k$  is shown for different values of  $\mu$ .

### III. RESULTS

#### A. Performance Analysis

To test the filter performance, an actual ICG wave, without any noise, is necessary. However, until now, we have not seen any work that deals with this standard ICG signal. In this way, computer simulations were carried out to evaluate the filter performance, using a triangular waveform  $s_k$  as the signal of interest, added to a noise  $n_k$ . At the  $k$ -th iteration  $s_k$  is defined as

$$s_k = \begin{cases} \frac{2A_s(k-mT)}{T}; & mT \leq k < mT + \frac{T}{2} \\ \frac{2A_s(T-(k-mT))}{T}; & mT + \frac{T}{2} \leq k < mT + T \end{cases} \quad (11)$$

where  $m = 0, 1, \dots, N-1$  is the recurrence number index,  $T$  is the period that yields  $f_s = 1/T$ , and  $A_s$  is the amplitude. The noise  $n_k$  was superimposed using a simulated respiratory artifact  $r_k$ , a simulated movement artifact  $m_k$ , and a random noise  $N_k$ , such as

$$\begin{cases} r_k = \sum_{i=1}^R \frac{A_r}{i} \sin(2\pi f_r k i) \\ m_k = \sum_{i=1}^M \frac{A_m}{i} \sin(2\pi f_m k i) \\ N_k = A_n \hat{n}_k \end{cases} \quad (12)$$

where  $\hat{n}_k$  is a uniformly distributed  $(0, 1)$  random sequence. The signals  $r_k$  and  $m_k$  are composed of a fundamental frequency  $f_r$  and  $f_m$ , respectively, and their correspondent harmonics with amplitudes decreasing exponentially. The signals  $s_k$ ,  $r_k$ , and  $m_k$  have an almost periodic behavior. This means that their fundamental frequencies  $f_s$ ,  $f_r$ , and  $f_m$ , respectively, vary randomly around one constant frequency. The primary input is then given by  $d_k = s_k + n_k = s_k + N_k + r_k + m_k$ . An example of the simulation output for different values of  $\mu$  is shown in Fig. 2.

The frequency  $f_s$  of the standard signal  $s_k$  was changed from 0.6 Hz to 2.0 Hz for the same noise  $n_k$ . Fig. 3 shows one example of the misadjustment behavior. We can observe a peak when the noise frequency lies in the same frequency as the standard signal. This is expected since it was assumed that the noise should be uncorrelated to the signal. For the other frequency values, we see that  $\mathbf{M} = \mu$  is a good approach since the misadjustment is around  $\mu = 0.05$ . The same behavior was observed for different signal and noises, though the MSE increased with the noise amplitude.

#### B. Spectral Analysis of Human Data

In order to test the performance of the SFLC, experiments were carried out, during rest and exercise, using an impedance plethys-

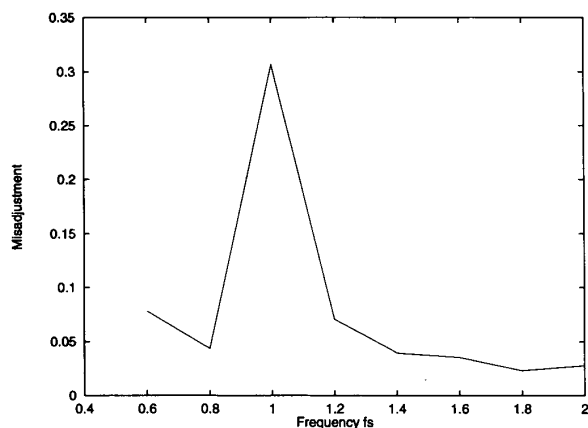


Fig. 3. The misadjustment for  $\mu = 0.05$ ,  $f_r = 0.32$ – $0.35$  Hz,  $f_m = 0.89$ – $1.13$  Hz,  $A_r = A_m = 0.3$ ,  $k = 9000$ ,  $M = R = 4$ . Note the peak when the noise frequency coincides with the signal frequency. For the other frequency values,  $M = \mu$  is a good approach.

mograph (model AI-601G, Nihon-Koden, Japan). Three electrodes were placed around the neck and four around the thorax. The inner electrodes were attached around the neck 2–3 cm below the source electrodes, and around the thorax 4 cm above the outer electrodes. The ECG was recorded with a bipolar lead from the thorax.

It is well known that the breathing and movement artifacts cause distortions in ICG wave. In this way, a metronome was used to set the breathing and movement artifacts in different fundamental frequencies.

Three normal subjects pedaled on a Monark 668 ergometer bicycle with a metronome set at a frequency of 120 bips/min, with loads of 30, 60, and 90 W exercise in such a way that the respiration was controlled at 20 or 30 times/min and pedaling at 60 times/min. During rest, there was no synchronization. The data were recorded for 3 min after 3 min of exercise in a TEAC RD-120TE DAT data recorder, and then sampled at a frequency of 100 Hz using an A/D converter with a 16-b NEC computer.

The data spectra were calculated using the FFT algorithm. For all data, the major spectrum lies below 10 Hz. Fig. 4 shows an example of the power spectra in one subject at 60 W exercise. It can be seen that the peak in the power spectrum occurs at the fundamental frequency corresponding to the R-R interval. As we can perceive, the filter attenuates the respiratory and movement artifact components occurring at 0.5 Hz (A) and 1.0 Hz (B), respectively, and also the movement artifacts harmonics occurring between the cardiac harmonics (D) and (F).

The data in the resting condition showed similar behavior, though no movement artifacts were observed. Moreover, the filter could not distinguish the movement artifact noises from the ICG signal when they were frequency coincident.

We have assumed that the signal has a limited bandwidth up to a certain harmonic  $H$ , allowing it to be recovered by a Fourier series limited to  $2H$  parameters. We see that the approximation fits well, since the major data power spectra lie in a limited bandwidth. An advantage of this approximation is that 50–60 Hz electrical interferences are eliminated. Fig. 5 shows the same data as a function of time.

#### IV. DISCUSSION AND CONCLUSION

Various works have been done to recover the signal in impedance cardiography produced only by the cardiac status. First, breath

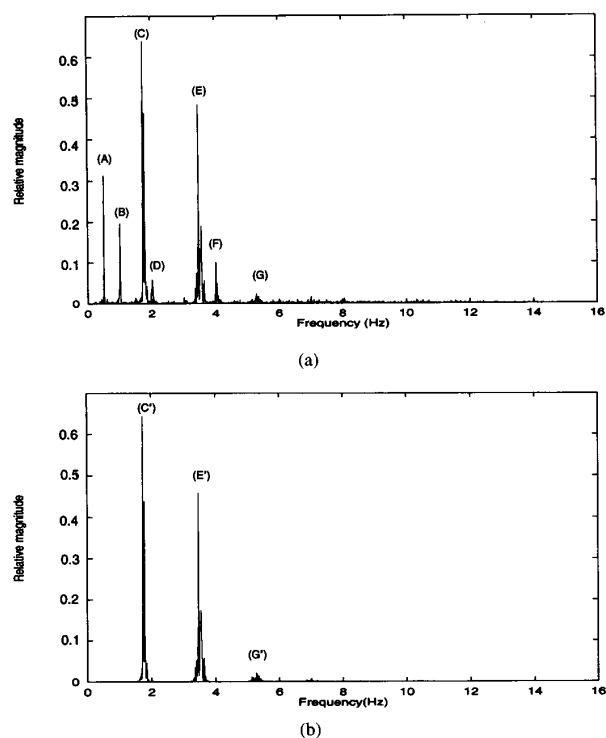


Fig. 4. The data power spectra obtained from a subject during 60 W exercise. (a) Raw data. (b) Filtered data with  $\mu = 0.05$ ,  $H = 15$ . The same data are shown in Fig. 5 in the field of time.

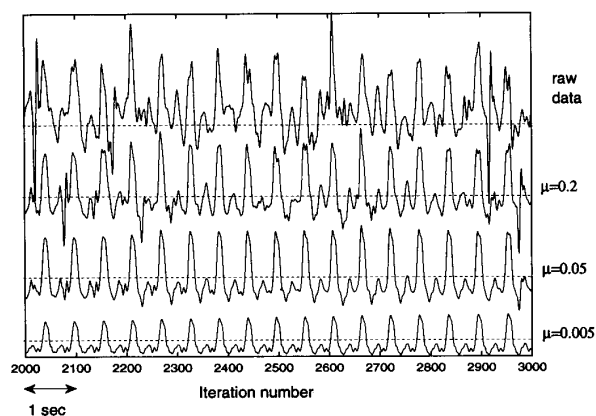


Fig. 5. An example of the filter output for data obtained at 60 W exercise.  $H = 15$ . Note that the smaller the step-size  $\mu$ , the slower the convergence. For example, the tracking capability for  $\mu = 0.005$  is quite slow.

holding was suggested, but it alters the stroke volume measurements. Then, ensemble averaging was proposed; however, it is not useful because the variation of R-R interval with the respiratory cycle may smear the  $dZ/dt$  peak. Also, high-pass and band-pass filters have been implemented, but the noises have a possibility of appearing inside the passing band of those filters.

A scaled Fourier linear combiner to impedance cardiographic signals event-related to the ECG R-R interval has been proposed. This filter is based on the property of a signal to be expressed as a sum of sines and cosines in a Fourier series in a period  $T$  determined

by the R-R interval. It estimates the coefficients in the Fourier series using the LMS algorithm. Instead of using a Fourier linear combiner (FLC) in the way proposed by Vaz and Thakor [14], we have used a scaling factor  $\frac{1}{\sqrt{H}}$  which leads to the step size  $\mu$  obeying the condition  $0 < \mu < \frac{1}{3}$  (refer to (9)) to assure the convergence of the LMS algorithm. While in the FLC, with the input correlation matrix  $R = (1/2)I$  (refer to [14, (4)]), the condition of convergence would depend on the number of weights, or  $0 < \mu < \frac{1}{3H}$ . This means that our method has more flexibility in choosing  $\mu$  than the FLC. Moreover, in the SFLC, the period  $T$  in the Fourier series is varying with the R-R interval, while in the FLC, a constant period  $T$  is assumed for all recurrences. With this assumption, a low-pass filtering effect may occur, caused by misalignment errors in the estimation. Thus, in this aspect, our method is better than the FLC.

The SFLC has the form of an on-line algorithm but cannot be carried out in an on-line manner, because at the  $m$ -th beat, we have not obtained the length of  $L_m$  yet. Thus, the computation should be carried out off-line or start at the beginning time of  $(m+1)$ -th beat. In this case, until the  $(m+1)$ -th beat had started, all that can be done is to store the  $m$ -th beat data. If the computer speed is fast enough, within the sampling intervals in the  $(m+1)$ -th beat, we may calculate the  $m$ -th beat data. At the  $k$ -th iteration in the  $m$ -th beat, which corresponds to the calculation to be carried out within  $(m+1)$ -th beat, the equation to obtain the output  $y_k$  (see (2)) needs  $2H$  times of multiplication because the number of elements of  $X_k$  or  $W_k$  is  $2H$ . This implies that the equation needs the computational time with the order of  $o(H)$ , where  $o(H)$  means that the number of operations are linearly dependent on  $H$ . In the same way, the LMS algorithm (6) needs computational time with the order of  $o(H)$ . On the other hand,  $x_{i,k}$ , which are the elements of  $X_k$ , needs  $2H$  times computation for calculating the function of sine or cosine for  $i = 1, 2, 3, \dots, 2H$  at the  $k$ -th iteration. Consequently, the computational time carried out at the beginning of the  $(m+1)$ -th beat depends on  $o(HL_m)$  because the size of the data to be processed at this time is  $L_m$ .

The advantage of using the SFLC is that it can reduce the influences of noises occurring between the signal harmonics, and the weights can be adjusted in a beat-by-beat basis, allowing a dynamic adaptation to the variations in the signal. Furthermore, the SFLC algorithm is quite simple to implement since the reference inputs (1) are different from one another only by an integer  $i$ .

There is a trade-off in choosing the value of  $\mu$  between the convergence time  $\tau_{mse}$  and the desired misadjustment  $M$  that will depend on the application. If a better performance in steady-state is important, a small  $M$  should be chosen, implying a smaller step size  $\mu$ . On the other hand, the signal may include a transient component, for example, during exercises where the load changes with time. In such a case, a faster convergence would be desirable in order to estimate this component. Thus, a larger  $\mu$  is required. Therefore, the choice of  $\mu$  is a compromise between less MSE and fast convergence.

However, if the periodicity of movement artifacts is the same as that of the cardiac signal, the misadjustment error increases sensitively, as observed in computer simulations. Therefore, care should be taken when choosing the breathing and movement artifact

frequencies in a way that they do not coincide with the cardiac artifact frequency.

As the signal is band-limited, the SFLC is useful because of its simplicity, lack of phase distortion, small data storage, and short computational time. Unfortunately, no referential data were available to compare the SFLC performance with other methods in directly measuring the human stroke volume.

## REFERENCES

- [1] N. J. Bershad, "On the optimum gain in LMS adaptation," *IEEE Trans. Acoust., Speech, Signal Processing*, vol. ASSP-35, pp. 1065-1068, 1987.
- [2] J. Chen, J. Vandewalle, W. Snasen, G. Vantrappen, and J. Janssens, "Adaptive method for cancellation of respiratory artifact in electrographic measurements," *Med. Biol. Eng. Comput.*, pp. 57-63, 1989.
- [3] O. Eiken and P. Segerhammar, "Elimination of breathing artifacts from impedance cardiograms at rest and during exercise," *Med. Biol. Eng. Comput.*, pp. 13-16, 1988.
- [4] M. Ferrigno, D. D. Hickey, M. H. Liner, and C. E. G. Lundgren, "Cardiac performance in humans during breath holding," *J. Appl. Physiol.*, vol. 60, pp. 1871-1877, 1986.
- [5] A. Feuer and E. Weinstein, "Convergence analysis of LMS filters with uncorrelated Gaussian data," *IEEE Trans. Acoust., Speech, Signal Processing*, vol. ASSP-33, pp. 222-230, 1985.
- [6] P. Laguna, R. Janè, O. Meste, P. Poon, P. Caminal, H. Rix, and N. V. Thakor, "Adaptive filter for event-related bioelectric signals using an impulse correlated reference input: Comparison with signal averaging techniques," *IEEE Trans. Biomed. Eng.*, vol. 39, pp. 1032-1043, 1992.
- [7] R. Janè, P. Laguna, N. V. Thakor, and P. Caminal, "Adaptive estimation of event-related bioelectric signals: Effect of misalignment errors," in *Proc. 13th Int. Conf. IEEE Eng. in Med. and Biol. Soc.*, pp. 365-366, 1991.
- [8] W. G. Kubicek, R. P. Patterson, J. N. Darnegis, D. A. Witsoe, and R. H. Mattson, "Development and evaluation of an impedance cardiac output system," *Aerospace Med.*, vol. 37, pp. 1208-1212, 1966.
- [9] M. Muzi, T. J. Ebert, F. E. Tristani, D. C. Jeutter, J. A. Barney, and J. J. Smith, "Determination of cardiac output using ensemble-averaged impedance cardiograms," *J. Appl. Physiol.*, vol. 58, pp. 200-205, 1985.
- [10] R. P. Patterson, W. G. Kubicek, E. Kinnen, D. A. Witsoe, and G. Noren, "Development of an electrical impedance plethysmography system to monitor cardiac output," in *Proc. 1st Annu. Rocky Mt. Bioeng. Sympos.*, U.S. Air Force Academy, Colorado Springs, pp. 56-71, 1964.
- [11] M. C. du Quesnay, G. J. Stoute, and R. L. Hughson, "Cardiac output in exercise by impedance cardiography during breath holding and normal breathing," *J. Appl. Physiol.*, vol. 62, pp. 101-107, 1987.
- [12] L. R. Rabiner and B. Gold, *Theory and Application of Digital Signal Processing*. Englewood Cliffs, NJ: Prentice-Hall, 1975.
- [13] S. B. Raza, R. P. Patterson, and L. Wang, "Filtering respiration and low-frequency movement artifacts from the cardiogenic signal," *Med. and Biol. Eng. and Comput.*, pp. 556-561, 1992.
- [14] C. Vaz and N. V. Thakor, "Adaptive Fourier estimation of time-varying evoked potentials," *IEEE Trans. Biomed. Eng.*, vol. BME-36, pp. 448-455, 1987.
- [15] B. Widrow and S. D. Stearns, *Adaptive Signal Processing*. Englewood Cliffs, NJ: Prentice-Hall, 1985.
- [16] L. R. Wang, P. Patterson, and S. B. Raza, "Respiratory effects on cardiac related impedance indices measured under voluntary cardiorespiratory synchronization (VCRS)," *Med. and Biol. Eng. and Comput.*, pp. 505-510, 1991.
- [17] Y. Yamamoto, K. Mokushi, S. Tamura, Y. Mutoh, M. Miyashita, and H. Hamamoto, "Design and implementation of a digital filter for beat-by-beat impedance cardiography," *IEEE Trans. Biomed. Eng.*, vol. 35, pp. 1086-1090, 1988.